

**Dieses Dokument ist eine Zweitveröffentlichung (Verlagsversion) /
This is a self-archiving document (published version):**

Feng Liu, Lei Zhang, Yue Zhang, Stefan C. B. Mannsfeld, Thomas P. Russell, Alejandro L. Briseno

Interpenetrating morphology based on highly crystalline small molecule and PCBM blends

Erstveröffentlichung in / First published in:

Journal of Materials Chemistry C. 2014, 2(44), S. 9368 - 9374 [Zugriff am: 04.11.2019]. Royal Society of Chemistry. ISSN 2050-7534.

DOI: <https://doi.org/10.1039/c4tc01451k>

Diese Version ist verfügbar / This version is available on:

<https://nbn-resolving.org/urn:nbn:de:bsz:14-qucosa2-362605>

„Dieser Beitrag ist mit Zustimmung des Rechteinhabers aufgrund einer (DFGgeförderten) Allianz- bzw. Nationallizenz frei zugänglich.“

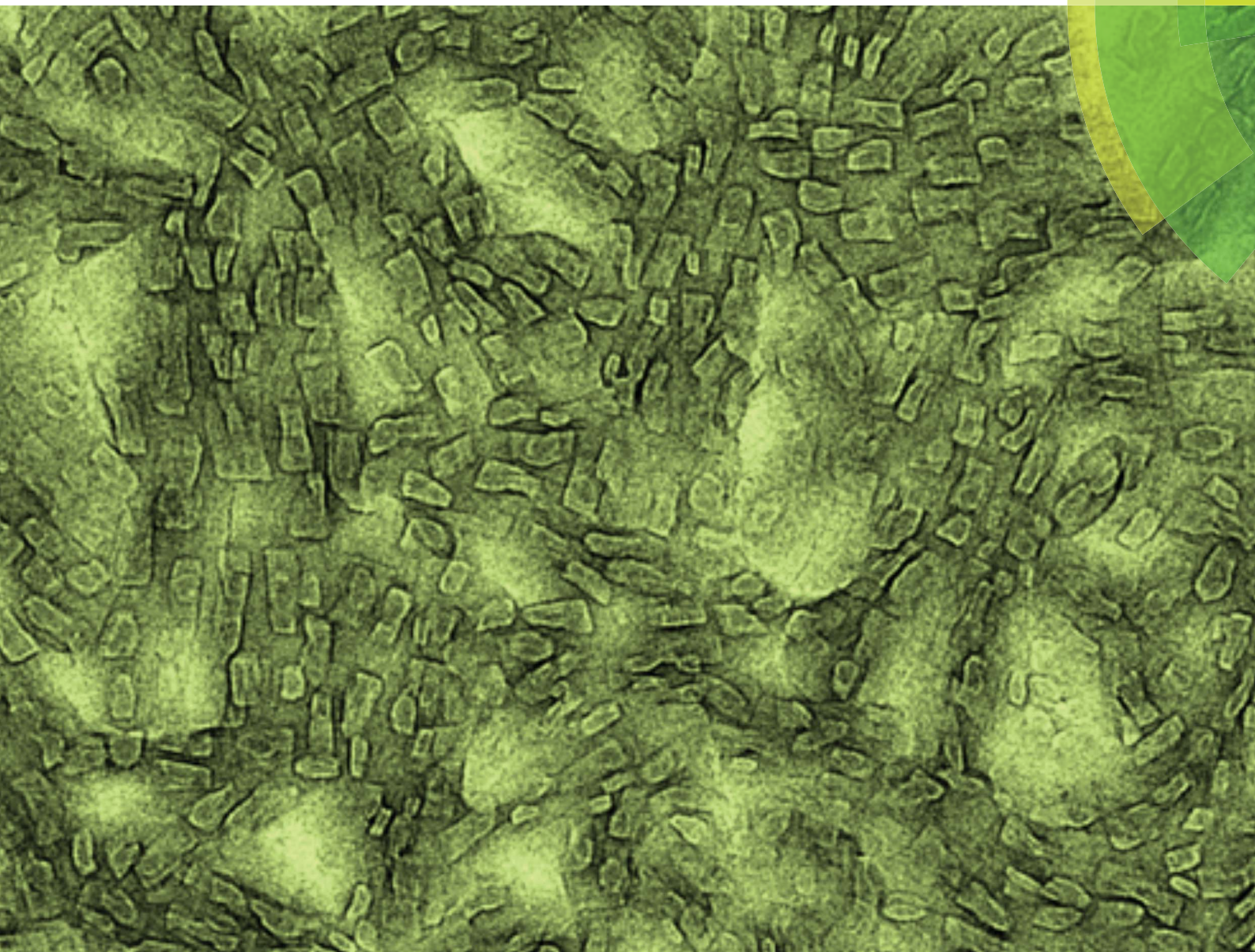
This publication is openly accessible with the permission of the copyright owner. The permission is granted within a nationwide license, supported by the German Research Foundation (abbr. in German DFG).

www.nationallizenzen.de/

Journal of Materials Chemistry C

Materials for optical, magnetic and electronic devices

www.rsc.org/MaterialsC



ISSN 2050-7526



PAPER

Thomas P. Russell, Alejandro L. Briseno *et al.*
Interpenetrating morphology based on highly crystalline small molecule
and PCBM blends

CrossMark
click for updatesCite this: *J. Mater. Chem. C*, 2014, 2, 9368Received 4th July 2014
Accepted 31st August 2014

DOI: 10.1039/c4tc01451k

www.rsc.org/MaterialsC

Interpenetrating morphology based on highly crystalline small molecule and PCBM blends†

Feng Liu,^a Lei Zhang,^a Yue Zhang,^a Stefan C. B. Mannsfeld,^b Thomas P. Russell^{*a} and Alejandro L. Briseno^{*a}

We report the morphological characterization of triisopropylsilylethynyl-dibenzochrysene (TIPS-DBC:PCBM) blends, a bulk heterojunction (BHJ) solar cell system based on a highly crystalline small molecule donor. We found that processing the blends from a volatile solvent such as chloroform is beneficial in controlling the crystal size and phase separation of the donor–acceptor phases. When a less-volatile solvent such as chlorobenzene is used, large crystalline domains formed, exceeding the length scale suitable for BHJ solar cells. When the BHJ films are thermally annealed, enhanced domain purity is observed for the chloroform processed thin films, which led to an increased short circuit current in the devices.

1. Introduction

Bulk heterojunction organic photovoltaics (OPV) have made major advances over the last two decades due to new material developments, optimization and device engineering.¹ Efficiencies higher than 10% have been demonstrated.² In BHJ OPVs, the morphology of the active layer consists of interpenetrating networks of donor and acceptor phases, where length scales of tens of nanometers are critical.³ Various factors, such as chemical structure, solubility, and crystallinity strongly influence the BHJ morphology.⁴ Processing conditions, such as solvent choice, thermal and solvent annealing, chemical additives, and film-casting methods, are important for controlling the morphology.⁵ Advances in characterization tools have provided insights into the morphology of the active layer, improving our understanding of the morphology–property relationship.^{6,7} Yet, our comprehension of this relationship is still far from complete. While crystalline domains influence exciton and hole transport, quantifying the interconnectivity of the crystalline domains has yet to be achieved. The nature of the amorphous domain,^{8–10} and how and to what extent PCBM mixes with the amorphous phase have only been speculated, but is of fundamental importance for exciton dissociation. There have been some models put forth,^{11–13} but a unified morphology–performance relationship has yet to emerge.

Small molecule BHJ OPVs,^{14–17} have recently gained more attention from a molecular design viewpoint and have shown an enhanced performance.^{18–34} Small molecules are very different from polymers, both in chemical structure and physical properties, but similar absorption features can be obtained in both material categories.³⁵ The differences in electronic structures between polymers and small molecules do affect their respective device performances. Parameters like the viscosity, crystallinity, and crystal orientation, are significantly different between these two categories of materials, which lead to a quite different optimized processing conditions for BHJ morphology.³⁶ As with polymer-based OPV, developing a structure–property relationship for small molecule organic photovoltaics is key in advancing their performance. Currently, high efficiency small molecule OPVs use conjugated oligomers, up to several thousand in molecular weight, and there is really no clear-cut physical property difference when compared to conjugated polymers.^{21,24,29,37} To gain insight into the structure–property relationship we revisited small molecules of a few hundreds of molecular weight,^{17,32} specifically a simple polycyclic aromatic hydrocarbon compound, triisopropylsilylethynyl-dibenzochrysene (TIPS-DBC) which was shown previously to be useful as a BHJ OPV with relatively good performance.³⁸ TIPS-DBC has a molecular weight of 660, is highly crystalline, can be processed in common solvents, like chloroform, and shows a device efficiency of around 2%. Here, we present a morphological characterization of TIPS-DBC to understand how solvents affect the structure–property relationship of this small molecular based BHJ OPV.

2. Results and discussions

The molecular structure, optical microscope images of crystals crystal packing, and UV-vis absorption spectra of TIPS-DBC are

^aDepartment of Polymer Science and Engineering, Conte Polymer Research Center, University of Massachusetts, 120 Governors Drive, Amherst, MA, 01003, USA. E-mail: abriseno@mail.pse.umass.edu; Russell@mail.pse.umass.edu

^bDresden University of Technology, Center for Advancing Electronics, 01062 Dresden, Germany

† Electronic supplementary information (ESI) available: Experimental details and portions of the experimental data of RSoXS, GIXD included. See DOI: 10.1039/c4tc01451k

shown in Fig. 1. TIPS-DBC has an aromatic core and a bulky solubilizing group, which is known to change crystal packing and impart solubility in oligoacenes.^{12,17} As shown in Fig. 1, TIPS-DBC recrystallized as large red needles and exhibited a slipped one-dimensional π -stacking motif, which is similar to that observed for some pentacene derivatives, with a distance of about 3.41 Å between molecules in the stacks.³⁹ However, the intermolecular surface overlap (about 5.64 Å²) is smaller than that of TIPS-pentacene (about 7.73 Å²) and the theoretical calculation indicates that significant coupling is found only along the *b*-axis.⁴⁰ Although the charge transport along the *b*-axis is about 0.1 cm² V⁻¹ s⁻¹ (Fig. S1†), such a packing (1-D), as suggested by Anthony, is favorable for solar cells compared to 2-D packing motifs.³² The highly ordered arrangements make TIPS-DBC fundamentally different from its conjugated polymer counterparts, which often form nanofibrillar crystalline structures in BHJ blends.⁵ When TIPS-DBC:PCBM blends are cast from solvents, crystallization plays a major role in defining the morphology. As TIPS-DBC crystallizes, PCBM is effectively an impurity that will be excluded from the crystal at the growth front.⁸ Fig. 1c shows the UV-vis absorption of TIPS-DBC in chloroform solution and TIPS-DBC : PCBM blends (1 : 1 weight ratio) processed under different conditions. In solution, TIPS-DBC showed strong absorption around 320 and 490 nm, with well-resolved vibronic structures. The short wavelength absorption band comes from segments of aromatic cores. The 490 nm absorption band comes from the major HOMO to LUMO transitions. In thin film, the major absorption band red shifted largely to 520–540 nm, due to packing induced J aggregations. The vibronic structure ceased in solid states. It

should be noted that the 310 nm absorption band concurrence with the major absorption peak of PCBM, thus led to superposition in blends absorptions. Thin films cast from chlorobenzene show a slight red-shift in the lowest energy absorption peak in comparison to films cast from chloroform, indicating either a higher degree of crystallinity or tighter packed structures with better electronic communications, which is supported by the following grazing X-ray diffraction investigation. Thermal annealing at 100 °C for 10 minutes resulted in a small red-shift for the chloroform-cast film, but did not change the absorption of CB-processed thin film (Fig. S2†). These absorption features indicate that CB produced a material that had improved structural order in TIPS-DBC thin film blends.

OPV devices using TIPS-DBC : PCBM blends in a 1 : 1 weight ratio were cast from both chloroform and chlorobenzene solutions, with the results shown in Fig. 2. Chloroform-cast devices show a moderate efficiency of ~1.8%. The major limiting factor for this device was a low short circuit current (J_{sc}) of 4.7 mA cm⁻² with an open circuit voltage of 0.72 V. Taking into account the poor absorption of TIPS-DBC, this device performance is reasonable, and is consistent with previous reports for this and similar materials.^{15,17} Thermal annealing of the as-cast BHJ blends at 100 °C for 10 min slightly increased the J_{sc} , while maintaining a constant V_{OC} and fill factor (FF). The thin film surface morphology was examined by atomic force microscopy (Fig. 3). The as-cast film shows a smooth surface with an RMS roughness of 0.78 nm. A granular feature, ~20 nm in size, is observed throughout the entire film. Under thermal treatment, both the size and connectivity of these grains are increased. In contrast, thin film devices fabricated from CB did not function

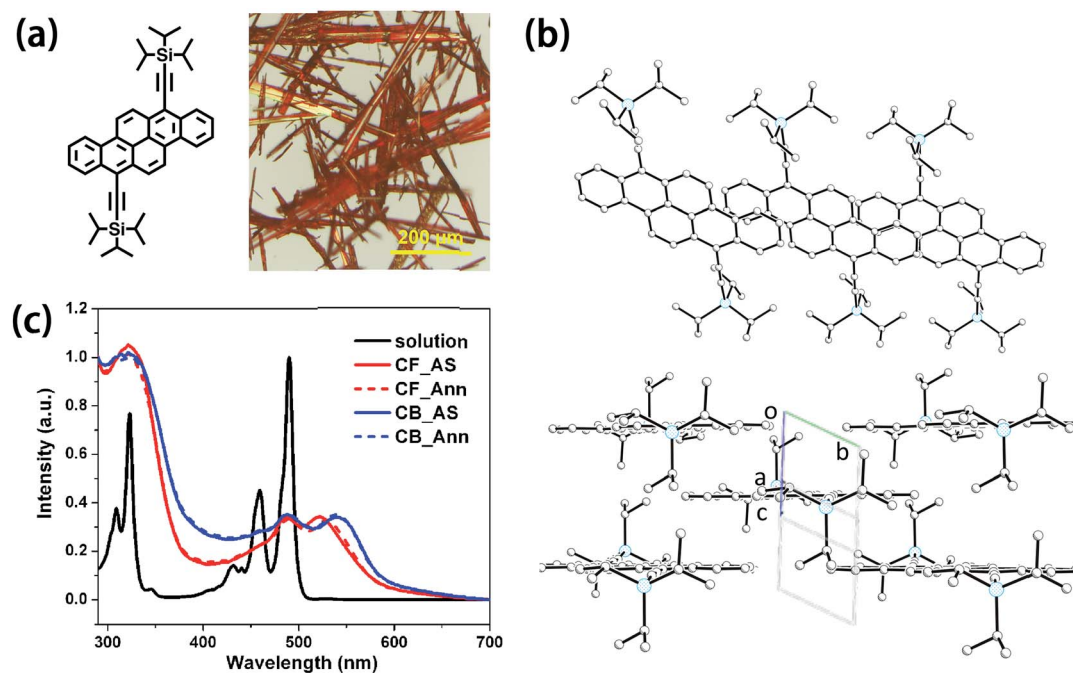


Fig. 1 (a) Molecular structure of TIPS-DBC and optical microscope image of needles-like crystals, (b) crystal structure showing the layered structure (top) and brick-layer packing (bottom). (c) UV-vis absorption of TIPS-DBC : PCBM (1 : 1 wt) blends processed from chloroform (CF) and chlorobenzene (CB) solvent under as spun (AS) and annealed (Ann) conditions. The annealing temperature is 100 °C.

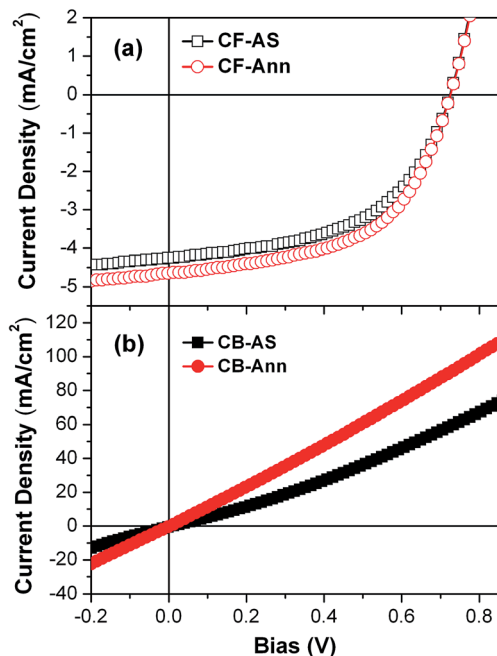


Fig. 2 Device performance of TIPS-DBC:PCBM OPV devices processed from two conditions with (a) chloroform, and (b) chlorobenzene solutions.

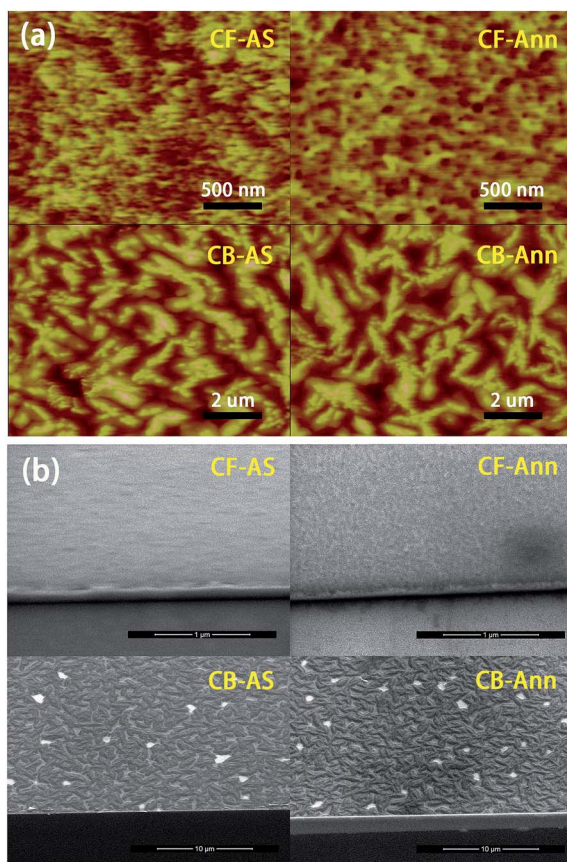


Fig. 3 AFM and SEM image of TIPS-DBC:PCBM blends.

properly. The J - V curve passes through the origin with a large current, indicating a short circuit. AFM analysis of the CB-cast thin film shows a surface with an RMS roughness of 11.2 nm. The surface morphology consists of isolated, micron-sized domains with heights of more than 80 nm, comparable to the total film thickness. Scanning electron microscopy (SEM) shows large pinholes between crystallites, giving a rational explanation of the non-functioning devices (ESI[†]). Thermal annealing (100 °C for 10 min) of the devices increased the current density, indicating that more pinholes or cracks were generated. This, more than likely, arises from the increase in the crystallinity of the TIPS-DBC.

The structure and orientation of the crystals on substrates were examined using grazing incidence wide-angle X-ray diffraction (GIXD).⁴¹ The GIXD spectrum (Fig. 4a) of the TIPS-DBC:PCBM thin films exhibit reflections characteristic of both TIPS-DBC crystallites and PCBM aggregates. TIPS-DBC forms highly-ordered crystallites on PEDOT:PSS coated substrates. A complete self-consistent indexing of the diffraction spots is possible but difficult due to a large number of weak broad reflections that form smeared-out streaks or are obscured by the broad halo from PCBM aggregates at $q \sim 1.38 \text{ \AA}^{-1}$. The in-plane unit cell can, however, be indexed as $|\mathbf{a}| = 7.47 \text{ \AA}$, $|\mathbf{b}| = 15.46 \text{ \AA}$, $\gamma = 81.6^\circ$, and the lamellar stacking distance $d_{001} = 17.16 \text{ \AA}$ is easily determined from the interferences along q_z at $q_y = 0$. Here we use the common surface lattice nomenclature which has the \mathbf{a} , \mathbf{b} vectors in the substrate plane. With the limited number of peaks it is difficult to unambiguously determine the alpha and beta angles of the unit cell. However, these \mathbf{a} , \mathbf{b} , γ parameters of the in-plane unit are quite similar to the $|\mathbf{a}|$, $|\mathbf{c}|$, β parameters of the bulk unit cell: $|\mathbf{a}| = 8.03 \text{ \AA}$, $|\mathbf{c}| = 16.36 \text{ \AA}$, $\beta = 81.8^\circ$, suggesting the possibility that TIPS-DBC grows in a structure similar to the bulk packing motif, but with the (010) crystal plane forming the basal plane (the plane in contact with the substrate). With the lamellar stacking distance d_{001} being 17.16 Å, the \mathbf{c} vector in our film is about double in length compared to its bulk counterpart ($|\mathbf{b}| = 8.43 \text{ \AA}$) which arises, more than likely, from an ABA type of stacking of (010) planes that leads to about twice as long repeat length as in the bulk unit cell. It needs to be noted that chloroform processed thin film blends showed extra diffraction peaks located around 0.45 \AA^{-1} and 0.9 \AA^{-1} in out-of-plane direction, indicating polymorph nature of the material. In the diffraction images in Fig. 4, PCBM shows a characteristic broad powder halo at 1.4 \AA^{-1} , a disordered packing of the PCBM.⁴² We also found that the crystallinity was higher for films cast from chlorobenzene, as evidenced the intensity and widths of the reflections (Fig. S4[†]). This is likely due to the lower vapor pressure of the chlorobenzene solvent, which evaporates more slowly than chloroform, allowing more time for the TIPS-DBC molecules to order and crystallize. The evaporation rate of chloroform during spin coating is sufficiently rapid that the crystal size is significantly reduced and both “edge on” and “face on” orientation is evident. From the GIXD results, TIPS-DBC assumes predominantly an edge-on orientation. Thermal annealing appears to improve the degree of crystallization of both the chloroform (CF) and chlorobenzene (CB) thin films, which is consistent with the UV-vis absorption measurements.

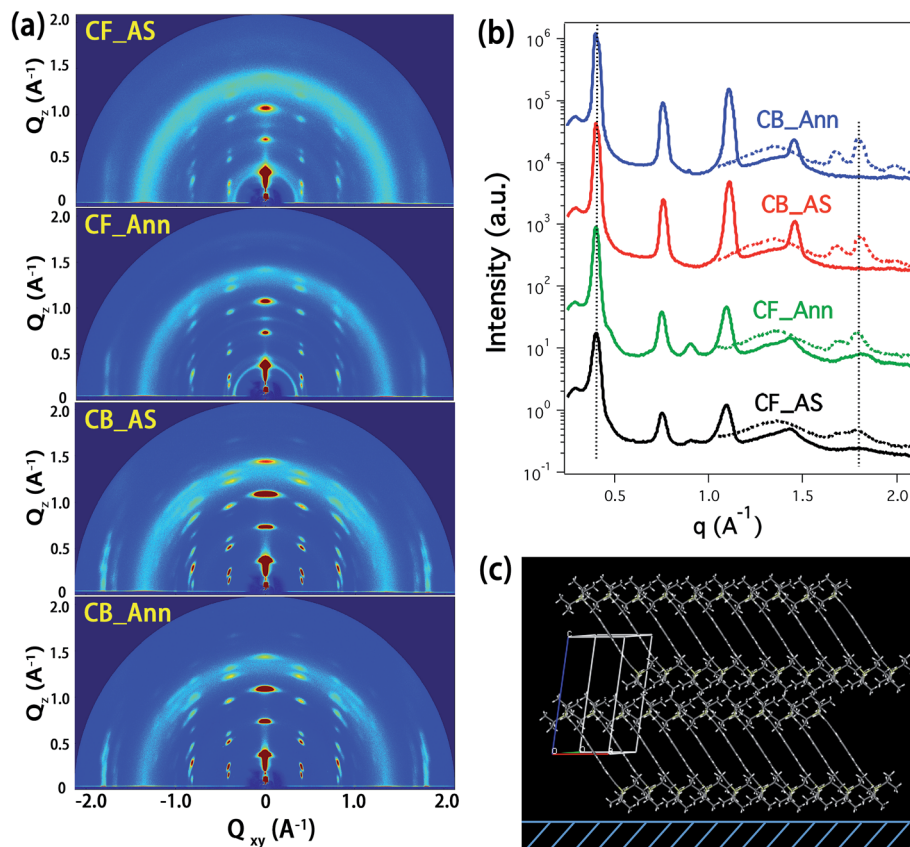


Fig. 4 (a) GIXD of TIPS-DBC:PCBM blends under different processing conditions, (b) line-cut profiles of the GIXD spectrums (solid line: out-of-plane cut, dashed line: in-plane cut), and (c) proposed crystal orientation of TIPS-DBC on the substrate.

The morphology of the blended thin films was also investigated by using transmission electron microscopy (TEM), with the results shown in Fig. 5. For films processed from CF (both as spun and annealed), an interpenetrated network structure is well defined. The lighter regions are ascribed to TIPS-DBC crystallites and the dark regions are PCBM rich domains due to their difference in electron densities. There is no evidence of large PCBM aggregation or segregation, indicating the TIPS-DBC crystalline network frames the morphology and prevents a large scaled aggregation or phase separation of PCBM aggregation.^{5,43} Thermal annealing enhances the crystallization of TIPS-DBC (as seen in the selected area electron diffraction profiles in the insets of Fig. 5), which also improves the purity of the PCBM-rich domains. This, more than likely, is the origin of the enhancement in the device performance. It should also be noted that the domain-to-domain spacing is ~ 60 nm, much larger than the optimal domain size for exciton diffusion,⁵ leading to a less-than-optimal interfacial area between the donor and acceptor and a lower short circuit current in devices. The effect of solvent choice is clearly seen from the morphology obtained by CB processing. Fig. 5c shows the as spun thin film, dark and light areas are seen due to mass-thickness contrast. Crystalline bricks of TIPS-DBC, having dimensions of 50×100 nm, are evident. The electron diffraction of the film shows strong reflections arising from the π - π stacking of TIPS-DBC

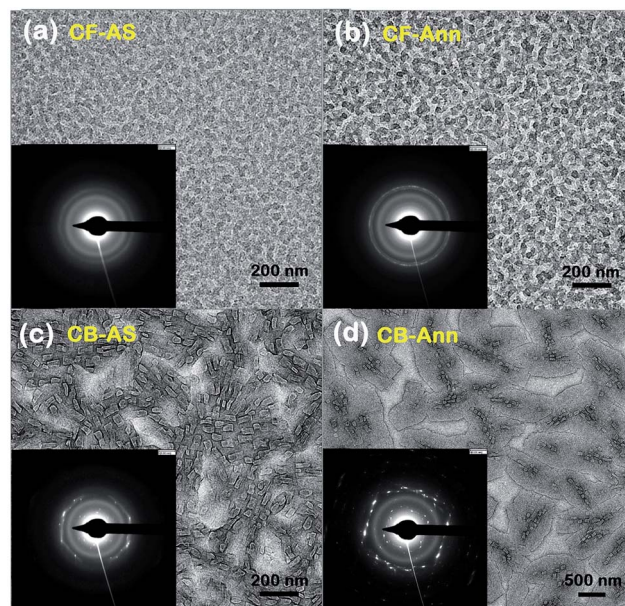


Fig. 5 Transmission electron microscopy images with corresponding electron diffraction patterns of TIPS-DBC:PCBM blends from chloroform (CF) solvent in (a) as spun (AS), (b) annealed (Ann), and from chlorobenzene (CB) solvent conditions, (c) as spun (AS), and (d) annealed (Ann). The diffraction pattern from both annealed conditions in (b) and (d) show a clear increase in crystallinity.

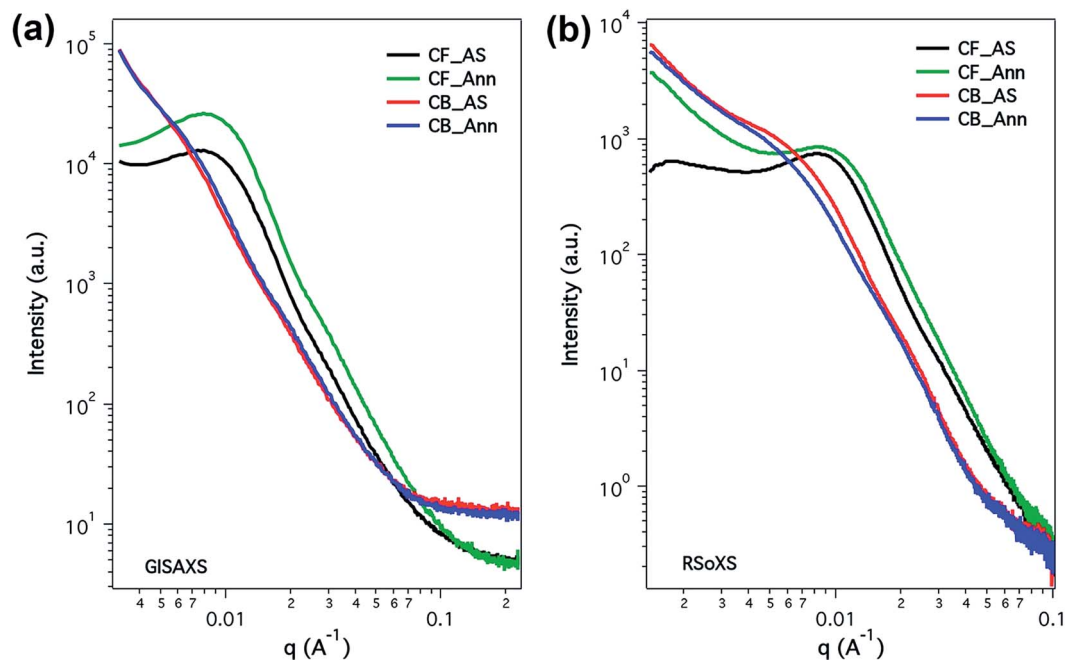


Fig. 6 GISAXS and RSoXS of TIPS-DBC:PCBM blends under different processing conditions.

With thermal annealing, large plate-shaped crystals formed from the melting and recrystallization of smaller crystal bricks. The molecules still adopt an edge-on orientation, as deduced from the GIXD and electron diffraction profiles.

Shown in Fig. 6 is grazing incidence small angle scattering (GISAXS) and the transmission resonant soft X-ray scattering (RSoXS) results of thin film blends prepared under different conditions.^{44,45} Results from these two methods agree well with each other and with the TEM observations. Both scattering methods demonstrate that the CF-processed BHJ thin films shown an interference at ~ 70 nm ($q = 0.009 \text{ \AA}^{-1}$), which corresponds to the average mesh size seen by TEM. CB-cast thin film blends show a shoulder in the scattering at $q \sim 0.008 \text{ \AA}^{-1}$ (corresponding to a distance of 78 nm), which corresponds to the average center-to-center distance between the crystalline “bricks” observed by TEM. With annealing, the scattering intensity increases slightly and the shoulder shifts to higher angles. This results from the melting and recrystallization process, where better-ordered crystals are formed and separation between the PCBM and the TIPS-DBC has increased. Quantifying the results further than this is difficult, due to the thickness variations in the film. The enhanced intensity in thermal annealed sample processed from chloroform indicates thermal annealing will increase the electron density fluctuation in the system, which will be direct measurement relative domain purity. If Iq^2 vs. q was plotted (GISAXS), the relative invariant by integrate the area under the curve will also give a measurement of relative domain purity.⁴⁶ It should be noted that the validity of this argument would require strict two-phase system, which our system presents. In fact, the previous TEM measurement of the thermal annealed sample processed from

chloroform gave a much clearer image, supporting the argument of the domain purity. When correlated with device function, we can conclude that relative domain purity could enhance the short circuit current in OPV devices, provided a similar general morphology is given. Thermal annealing of the CB processed blends drastically changed the morphological picture of the blends. The number density of crystalline bricks decreased and large plates of micrometer in size were seen. This was reflected in the reduced scattering shoulder in RSoXS. The formation of these thin plates did not cover the cracks in the thin film, thus the device still shorted. Current results in thin film morphology clearly point out the importance of solvent choice in optimizing device performance. When a new light absorbing material is obtained, it is necessary to try solvents of different volatility and polarity to get an idea of suitable base solvent. Then systematic optimizations can be carried out.

3. Conclusions

We have investigated the morphology of small molecular based BHJ solar cells. The studies indicate that processing solvents have a profound influence on the morphology of BHJ blends. For small molecules that have a high crystallinity, low viscosity, low boiling point solvents that rapidly evaporate and freeze the morphology in a suitable length scale are more favorable in device fabrication, as in the current system TIPS-DBC:PCBM blends. These features make chloroform works as the one important solvent in small molecule based OPVs. It should also be noticed that some new developed high performance small molecule OPV material, due to their solubility limit or different crystallization behaviors, form decent morphology when using high boiling point solvent to process, yielding remarkable

device performances. The use of solvent additive quickly emerged as an important method in morphology control, whose presence in solvents not only affects the crystallization of materials, but also influence the interaction of donor and acceptor materials, thus much more complicated than the current pure solvent processing discussion. The low PCE of TIPS-DBC based solar cells is expected due to its poor light absorption. However, it is a good model system to visualize the morphology of those small chromophore blends. The ~ 70 nm length scale of phase separation is far from optimized value, which further reduces short circuit current in devices. And this feature is critical in developing next generation of high performance small molecules. The TIPS-DBC:PCBM blends also serves as a good model system to directly visualize the domain purity and performance relationship, under the circumstances of thermal treatment, which can be extended in the future for similar systems.

4. Experimental

TIPS-DBC is obtained by synthesis following reported procedure.⁴⁰ PC₆₁BM (PCBM) was obtained from American Dye Source (Lot # 11F009E). BHJ devices were fabricated on ITO/PEDOT:PSS substrates. TIPS-DBC : PCBM = 1 : 1 weight ratio blend was prepared, and dissolved in chloroform or chlorobenzene solvents. ~ 100 nm thin films were prepared by spin coating to fabricate devices (for chloroform solvent, 4000 rpm spinning rate was used; for chlorobenzene solvent, 2000 rpm spinning rate was used). Thermal annealing (100 °C, 10 min) was carried out in N₂ filled glove box. LiF (1.5 nm)/Al (100 nm) was thermally deposited to complete the device.

GIXD was carried out at beamline 11-3 Stanford Synchrotron Light Source (SSRL). The sample was placed inside a helium chamber, and an image plate was used to collect the signal. GISAXS was carried out at beamline 7.3.3 Lawrence Berkeley National Lab (LBNL), using Pilatus 1M detector. The sample preparation was exactly the same with device preparation conditions, except using wafer as supporting substrates (also with PEDOT:PSS). RSoXS was performed at beamline 11.0.1.2 Lawrence Berkeley National Lab. Thin films were floated and transferred onto Si₃N₄ substrates and experiments were done in transmission mode.

Transmission electron microscopy studies were conducted with a JEOL 2000 FX TEM operating at an accelerating voltage of 200 kV. Scanning force microscopy was performed on a Digital Instruments Dimension 3100, operating in tapping mode. SEM was done on Magellan FEI 400L. Imaging was typically performed with electron energy of 2 keV. Thin film samples were spin-coated onto PEDOT:PSS coated wafers, followed by cooling in liquid N₂ for 5 minutes. Sample for Cross section SEM was fabricated by breaking the substrate.

Acknowledgements

This work was supported by the Department of Energy supported Energy Frontier Research Center at the University of Massachusetts (DOE DE-SC0001087). L.Z. and Y.Z thank the

Office of Naval Research (N000141110636) for support in synthesis and characterization of the donor compound. Portions of this research were carried out at the Advanced Light Source, Berkeley National Laboratory, and Stanford Synchrotron Radiation Lightsource, which was supported by the DOE, Office of Science, and Office of Basic Energy Sciences. The authors thank Ms Yue Wang for assistance with TEM.

References

- 1 C. J. Brabec, S. Gowrisanker, J. J. M. Halls, D. Laird, S. Jia and S. P. Williams, *Adv. Mater.*, 2010, **22**, 3839–3856.
- 2 J. You, L. Dou, K. Yoshimura, T. Kato, K. Ohya, T. Moriarty, K. Emery, C.-C. Chen, J. Gao, G. Li, *et al.*, *Nat. Commun.*, 2013, **4**, 1446.
- 3 F. Liu, Y. Gu, X. Shen, S. Ferdous, H.-W. Wang and T. P. Russell, *Prog. Polym. Sci.*, 2013, **38**, 1990–2052.
- 4 L. Bian, E. Zhu, J. Tang, W. Tang and F. Zhang, *Prog. Polym. Sci.*, 2012, **37**, 1292–1331.
- 5 F. Liu, Y. Gu, J. W. Jung, W. H. Jo and T. P. Russell, *J. Polym. Sci., Part B: Polym. Phys.*, 2012, **50**, 1018–1044.
- 6 D. M. DeLongchamp, R. J. Kline and A. Herzing, *Energy Environ. Sci.*, 2012, **5**, 5980.
- 7 W. Chen, M. P. Nikiforov and S. B. Darling, *Energy Environ. Sci.*, 2012, **5**, 8045–8074.
- 8 B. A. Collins, E. Gann, L. Guignard, X. He, C. R. McNeill and H. Ade, *J. Phys. Chem. Lett.*, 2010, **1**, 3160–3166.
- 9 B. A. Collins, J. R. Tumbleston and H. Ade, *J. Phys. Chem. Lett.*, 2011, **2**, 3135–3145.
- 10 M. A. Ruderer, R. Meier, L. Porcar, R. Cubitt and P. Müller-Buschbaum, *J. Phys. Chem. Lett.*, 2012, **3**, 683–688.
- 11 D. Chen, F. Liu, C. Wang, A. Nakahara and T. P. Russell, *Nano Lett.*, 2011, **11**, 2071–2078.
- 12 D. Chen, A. Nakahara, D. Wei, D. Nordlund and T. P. Russell, *Nano Lett.*, 2011, **11**, 561–567.
- 13 W. Yin and M. Dadmun, *ACS Nano*, 2011, **5**, 4756–4768.
- 14 Y. Chen, X. Wan and G. Long, *Acc. Chem. Res.*, 2013, **46**, 2645–2655.
- 15 J. E. Coughlin, Z. B. Henson, G. C. Welch and G. C. Bazan, *Acc. Chem. Res.*, 2014, **47**, 257–270.
- 16 J. Roncali, *Acc. Chem. Res.*, 2009, **42**, 1719–1730.
- 17 M. Lloyd, J. Anthony and G. Malliaras, *Mater. Today*, 2007, 1–8.
- 18 B. Walker, X. Han, C. Kim, A. Sellinger and T.-Q. Nguyen, *ACS Appl. Mater. Interfaces*, 2012, **4**, 244–250.
- 19 Z. Li, G. He, X. Wan, Y. Liu, J. Zhou, G. Long, Y. Zuo, M. Zhang and Y. Chen, *Adv. Energy Mater.*, 2012, **2**, 74–77.
- 20 Y. Liu, X. Wan, F. Wang, J. Zhou, G. Long, J. Tian, J. You, Y. Yang and Y. Chen, *Adv. Energy Mater.*, 2011, **1**, 771–775.
- 21 B. Walker, A. B. Tamayo, X.-D. Dang, P. Zalar, J. H. Seo, A. Garcia, M. Tantiwiwat and T.-Q. Nguyen, *Adv. Funct. Mater.*, 2009, **19**, 3063–3069.
- 22 A. Garcia, G. C. Welch, E. L. Ratcliff, D. S. Ginley, G. C. Bazan and D. C. Olson, *Adv. Mater.*, 2012, **24**, 5368–5373.
- 23 T. S. van der Poll, J. A. Love, T.-Q. Nguyen and G. C. Bazan, *Adv. Mater.*, 2012, **24**, 3646–3649.

- 24 Y. Liu, X. Wan, F. Wang, J. Zhou, G. Long, J. Tian and Y. Chen, *Adv. Mater.*, 2011, **23**, 5387–5391.
- 25 C. Kim, J. Liu, J. Lin, A. B. Tamayo, B. Walker, G. Wu and T.-Q. Nguyen, *Chem. Mater.*, 2012, **24**, 1699–1709.
- 26 J. Zhou, X. Wan, Y. Liu, G. Long, F. Wang, Z. Li, Y. Zuo, C. Li and Y. Chen, *Chem. Mater.*, 2011, **23**, 4666–4668.
- 27 J. Zhou, Y. Zuo, X. Wan, G. Long, Z. Qian, W. Ni, Y. Liu, Z. Li, G. He, C. Li, *et al.*, *J. Am. Chem. Soc.*, 2013, **135**, 8484–8487.
- 28 C. J. Takacs, Y. Sun, G. C. Welch, L. A. Perez, X. Liu, W. Wen, G. C. Bazan and A. J. Heeger, *J. Am. Chem. Soc.*, 2012, **134**, 16597–16606.
- 29 J. Zhou, X. Wan, Y. Liu, Y. Zuo, Z. Li, G. He, G. Long, W. Ni, C. Li, X. Su, *et al.*, *J. Am. Chem. Soc.*, 2012, **134**, 16345–16351.
- 30 Z. B. Henson, G. C. Welch, T. van der Poll and G. C. Bazan, *J. Am. Chem. Soc.*, 2012, **134**, 3766–3779.
- 31 Y. Matsuo, Y. Sato, T. Niinomi, I. Soga, H. Tanaka and E. Nakamura, *J. Am. Chem. Soc.*, 2009, **131**, 16048–16050.
- 32 M. T. Lloyd, A. C. Mayer, S. Subramanian, D. A. Mourey, D. J. Herman, A. V. Bapat, J. E. Anthony and G. G. Malliaras, *J. Am. Chem. Soc.*, 2007, **129**, 9144–9149.
- 33 A. B. Tamayo, M. Tantiwiwat, B. Walker and T.-Q. Nguyen, *J. Phys. Chem. C*, 2008, **112**, 15543–15552.
- 34 A. B. Tamayo, B. Walker and T.-Q. Nguyen, *J. Phys. Chem. C*, 2008, **112**, 11545–11551.
- 35 B. Walker, C. Kim and T.-Q. Nguyen, *Chem. Mater.*, 2011, **23**, 470–482.
- 36 B. Walker, A. Tamayo, D. T. Duong, X.-D. Dang, C. Kim, J. Granstrom and T.-Q. Nguyen, *Adv. Energy Mater.*, 2011, **1**, 221–229.
- 37 Y. Sun, G. C. Welch, W. L. Leong, C. J. Takacs, G. C. Bazan and A. J. Heeger, *Nat. Mater.*, 2011, **11**, 44–48.
- 38 K. N. Winzenberg, P. Kemppinen, G. Fanchini, M. Bown, G. E. Collis, C. M. Forsyth, K. Hegedus, T. B. Singh and S. E. Watkins, *Chem. Mater.*, 2009, **21**, 5701–5703.
- 39 J. E. Anthony, *Chem. Rev.*, 2006, **106**, 5028–5048.
- 40 L. Zhang, A. Fonari, Y. Zhang, G. Zhao, V. Coropceanu, W. Hu, S. Parkin, J.-L. Brédas and A. L. Briseno, *Chem.–Eur. J.*, 2013, **19**, 17907–17916.
- 41 J. Rivnay, S. C. B. Mannsfeld, C. E. Miller, A. Salleo and M. F. Toney, *Chem. Rev.*, 2012, **112**, 5488–5519.
- 42 M.-Y. Chiu, U.-S. Jeng, M.-S. Su and K.-H. Wei, *Macromolecules*, 2010, **43**, 428–432.
- 43 F. Liu, Y. Gu, C. Wang, W. Zhao, D. Chen, A. L. Briseno and T. P. Russell, *Adv. Mater.*, 2012, **24**, 3947–3951.
- 44 E. Gann, A. T. Young, B. A. Collins, H. Yan, J. Nasiatka, H. A. Padmore, H. Ade, A. Hexemer and C. Wang, *Rev. Sci. Instrum.*, 2012, **83**, 045110.
- 45 C. Wang, D. H. Lee, A. Hexemer, M. I. Kim, W. Zhao, H. Hasegawa, H. Ade and T. P. Russell, *Nano Lett.*, 2011, **11**, 3906–3911.
- 46 W. Ma, J. R. Tumbleston, M. Wang, E. Gann, F. Huang and H. Ade, *Adv. Energy Mater.*, 2013, **3**, 864–872.